Available online at www.sciencedirect.com

ScienceDirect

Radiation Physics and Chemistry 75 (2006) 2151–2158

Radiation Physics and Chemistry

www.elsevier.com/locate/radphyschem

Velocity map imaging for low-energy electron–molecule collisions

D. Nandi, V.S. Prabhudesai, E. Krishnakumar*

Tata Institute of Fundamental Research, Homi Bhabha Road, Colaba, Mumbai 400005, India

Received 12 November 2004; accepted 24 February 2006

Abstract

The development of an experiment for velocity map imaging (VMI) of fragment ions arising from electron–molecule collisions is discussed. The angular distribution of O^- from the dissociative attachment and dipolar dissociation of O_2 is measured and compared with the existing data. The details of the technique and its importance to electron–molecule collisions are discussed.

Keywords: Dissociative attachment; Dipolar dissociation; Velocity map imaging; Electron–molecule collisions

1. Introduction

Imaging of ions and electrons has become a versatile tool in atomic collision physics in recent times. By combining the use of appropriate magnetic and electric fields with a two-dimensional position sensitive detector, a host of new imaging techniques have been developed and used to obtain qualitatively new information in some of the atomic collision processes. Initially developed for ion–atom collision experiments, Recoil Ion Momentum Spectroscopy (RIMS) (Ullrich et al., 1991) and its variation using a cold target (COLTRIMS) (Dörner et al., 1997) have provided detailed dynamics atomic and molecular ionization under the influence of swift ion projectiles (Schulz et al., 2003), photoionization (Diez et al., 2004; Weber et al., 2004) and intense field ionization (Rottke et al., 2002). In these as well similar multi-particle coincidence experiments (Amitay and Zajfman, 1997; Helm et al., 1993) all the three momentum components of one or more particles are measured simultaneously to obtain the kinematic details of the collisions and to derive the corresponding physics. Velocity map imaging (VMI) is another charged particle imaging technique which had its origin in laser photodissociation experiments (Chandler and Houston, 1987; Eppink and Parker, 1997). Since then, this technique has been used extensively in many of its variations in reactive collisions, photodissociation, photodetachment and photoionization experiments (Whitaker, 2003) and improvements and modifications of this technique are continuing to appear (Gebhardt et al., 2001; Townsend et al., 2003; Dinu et al., 2002; Baguenard et al., 2004) All these techniques have been used in experiments where the charged particles, which are imaged, are created by either a high-energy projectile or a short pulse laser. This allows the use of appropriate electric/magnetic fields for the necessary imaging configuration, without worrying about its effect on the ionizing agent or the collision process. In contrast to this, the area of low-energy electron collisions has missed out on the advantages of these developments in charged particle imaging techniques. The major obstacle in this respect has been in

*Corresponding author. Tel.: +91 22 22782502; fax: +91 22 22804610.

E-mail address: ekkumar@tifr.res.in (E. Krishnakumar).

0969-806X/$ - see front matter © 2006 Elsevier Ltd. All rights reserved.
doi:10.1016/j.radphyschem.2006.02.016

providing an appropriate electric field configuration which does not affect the incoming low-energy projectiles, and the necessary time resolution to measure the velocity components accurately. In this context, we have developed a technique to carry out VMI of the ionic fragments produced in electron–molecule collisions.

The importance of electron–molecule collisions have long been appreciated for their role in large variety of applications and in other basic sciences. The basic aspect of all these applications is what is called "electron-induced chemistry". It is increasingly becoming evident that low-energy electron–molecule interactions with all its varied manifestations in inelastic processes like excitation, dissociation, ionization, dissociative ionization, dissociative attachment (DA) and dipolar dissociation are fundamental to the chemistry of various environments (Becker et al., 2000). These processes also play a major role in radiation-induced damage in biomolecules. It has been shown that DA of electrons below 10 eV is the most dominant channel through which damage to DNA occurs in the interaction of high-energy radiation with biological tissues (Boudaïffa et al., 2000). Despite their importance, due to inherent difficulties, detailed kinematical studies of various dissociation processes in electron–molecule collisions have been very limited. It may be of interest to note that reliable technique to measure partial cross-sections for dissociative ionization (Krishnakumar and Srivastava, 1992) and DA (Krishnakumar and Nagesha, 1992) in molecules by electron impact came into existence in not too distant past.

The dynamics of dissociative ionization and DA in electron–molecule collisions have been studied using kinetic energy spectrometry for several molecules. However, the angular distribution measurements have been rather limited. Anisotropy in angular distribution of fragment negative ions is characteristic of the DA process (Dunn, 1962). The angular distribution measurements allow one to determine the quantal state of negative ion resonance and the partial waves of the electrons that are captured (O'Malley and Taylor, 1968). The measurements reported till now on angular distributions have been carried out using the conventional turn-table arrangement and subsequently limited to finite angular range. Our motivation for the development of the VMI technique for electron–molecule collisions has been to measure the angular distribution in the entire 2π angle as well as to improve the sensitivity (and thus the data acquisition time) for experiments involving low cross-sections or small target densities as in the case of electron collisions on excited molecules (Krishnakumar et al., 1997; Rangwala et al., 2001).

Formation of fragment negative ions from molecules, through dipolar dissociation is a process common to both photoabsorption and electron impact excitation (or for that matter, collision of any particle with enough energy to excite the molecule to the appropriate states). The excited states of molecules which eventually break up through dipolar dissociation are states lying in the ionization continuum of the neutral molecules and hence are autoionizing states. Thus, autoionization and dipolar dissociation are competing channels for decay of these excited states. These states are also characterized by potential energy minima at large internuclear separations, due to the dipolar interaction. However, since the mimima are at large internuclear separations, they cannot be accessed by transitions from the ground states of the molecules. Any excitation to these states from the ground state of the molecule ends up at the repulsive part of their PE curves and thus lead to dissociation. Photoabsorption and photoionization experiments (Berkowitz, 1979) have shown the presence of these states in a number of molecules. Though photoabsorption experiments to study these states have the advantage of better energy resolution, electron impact excitation has the special benefit that it will not be limited by the dipole selection rules. Thus electron impact excitation is a more versatile technique for studying the dipolar dissociation process. However, except for measurements of integral cross-sections, very limited number of experiments has been carried to identify the states leading to dipolar dissociation and to detail their dynamics. We demonstrate below that the VMI of the negative ions produced by electron impact is an ideal technique to study the dipolar dissociation as well as DA.

2. Experiment

The experiment uses a magnetically collimated and pulsed electron gun, an effusive molecular beam target, and the VMI arrangement. A Faraday cup is used to monitor the electron current. The electron gun is of simple design using a heated tungsten filament to produce the electrons by thermionic emission, a cathode of Pierce geometry, a grid and finally a grounded aperture to which the electrons are accelerated from the negatively biased filament and cathode. The gun is pulsed by using a negative bias on the grid with respect to the filament and cathode and overriding it with a positive pulse of small duration. The magnetic field ($\sim$50 G) for collimating the electron beam is generated by a pair of large Helmholtz coils placed outside the vacuum chamber. The typical energy resolution of the electron beam from this gun is 0.5 eV. The magnetic collimation gives almost constant current from 1 eV onwards under optimum operating conditions.

The target molecular beam was produced by allowing the gas of interest to flow through a capillary array. The advantages of a capillary array for producing effusive beams of reasonably good quality for collision

experiments have been discussed before (Bapat and Krishnakumar, 1994, 1995). We estimate that the typical target pressure used in the current experiments were 10^{-4} Torr. This corresponded to an ambient pressure of 10^{-6} Torr in the vacuum chamber during the experiments. The vacuum chamber was pumped down to a pressure of low 10^{-9} Torr of by a 2000 l/s Turbo pump and oil free fore line pump before the experiments.

The ion optics for VMI along with the rest of the experimental arrangement is shown in Fig. 1. The ion optics consists of three electrodes and a relatively short flight tube. The ion extraction is provided by the electric field between the 'pusher' and the 'puller'. The lens electrode between the puller and the flight tube provides the appropriate velocity focusing at the detector. For the velocity mapping we have followed the time slicing principle employed by Gebhardt et al. (2001). In this arrangement, the ions are produced in a field free region. They are extracted out after they are allowed to bloom for a finite time interval. The extracted ions are velocity mapped onto a two-dimensional position sensitive detector employing microchannel plates, a phosphor screen and video camera. The time delayed extraction in their experiment allows the Newton sphere to expand both in the direction of flight as well as perpendicular to it. In the arrangement by Gebhardt et al. only the central thin slice of the Newton sphere parallel to the two-dimensional detector are detected, by pulsing the bias to the microchannel plates at a selected time. We found that this delayed extraction of ions followed by time-slicing with suitable modifications, is the most appropriate method for velocity mapping of ions produced by electron collisions. We employed electron pulses of width 200 ns and extracted the ions after a delay of additional 200 ns using a negative pulse of 22 V applied to the pusher plate. The rest of the electrodes were biased appropriately for velocity mapping condition.

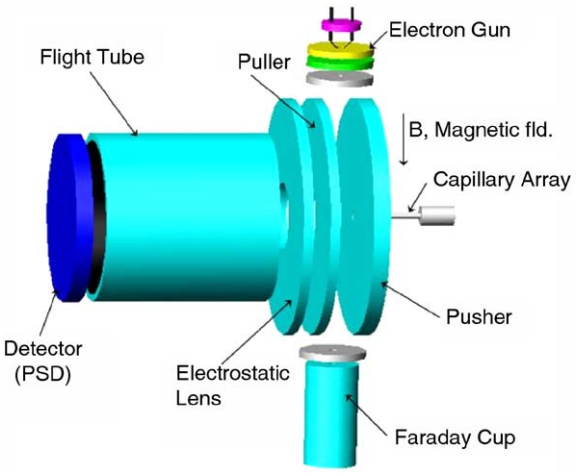

Fig. 1. Schematic of the experimental arrangement.

The ions were detected using a Z-stack microchannel plate assembly of 50 mm diameter. The position information was obtained using a Wedge and Strip anode. For each ion detected, its position and time of arrival were recorded separately using the list mode data acquisition using the LAMPS program (Chatterjee) running on Linux operating system. The offline data analysis is also carried out using this program.

3. Measurements on O_2

To begin with, the angular distribution of O^- from O_2 by DA was measured. The DA from O_2 is known to occur as a broad peak centered at 6.5 eV. The dissociation limit for the observed resonance is known to

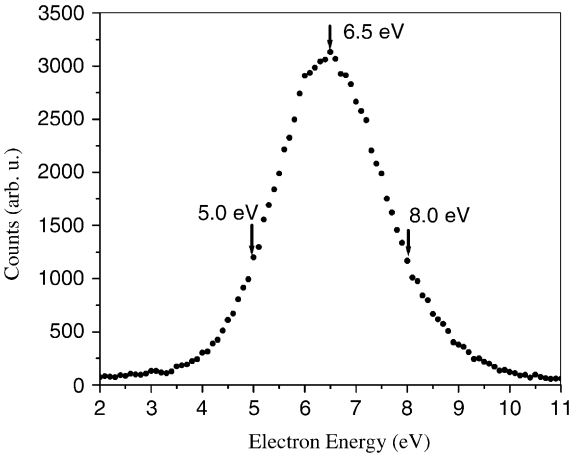

Fig. 2. Ion yield curve of O^- from O_2 by dissociative attachment.

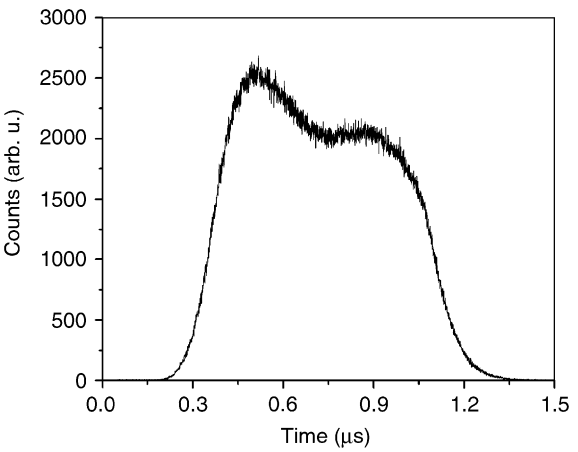

Fig. 3. Time-of-flight spectrum of O^- from dissociative attachment to O_2.

correspond to both the O^- and O fragments in their ground states. The angular distribution of O^- from this process has been measured earlier using the conventional technique in the range of 20–160°. The ion yield curve for O^- from O_2 obtained by us is shown in Fig. 2. The arrows indicate the energies at which the VMI measurements were made. A typical time-of-flight spectrum of the O^- ions is shown in Fig. 3. The asymmetry of the peak is believed to be due to differing field conditions that the ions ejected towards the flight tube and away from the flight tube experienced. This difference does not hamper our measurements, since we are interested only in the central part of the time-of-flight spectrum. This central section corresponds to ions ejected in the plane perpendicular to the time-of-flight axis and contains all the velocity information that we seek to obtain. The VMI data obtained from the central part of the time-of-flight spectra at three different electron energies are shown in Fig. 4. The direction of the electron beam is vertically down in all the cases. The figure also shows the distributions of intensity as a function of the position on the detector at these energies. These velocity map images show that ions are produced with a specific energy, but their directions are not isotropic. The diameter of the ring like pattern should be proportional to the initial speed of the ions. In principle, we should be able to use the ring diameter to determine the initial kinetic energy of the ions. We find that due to

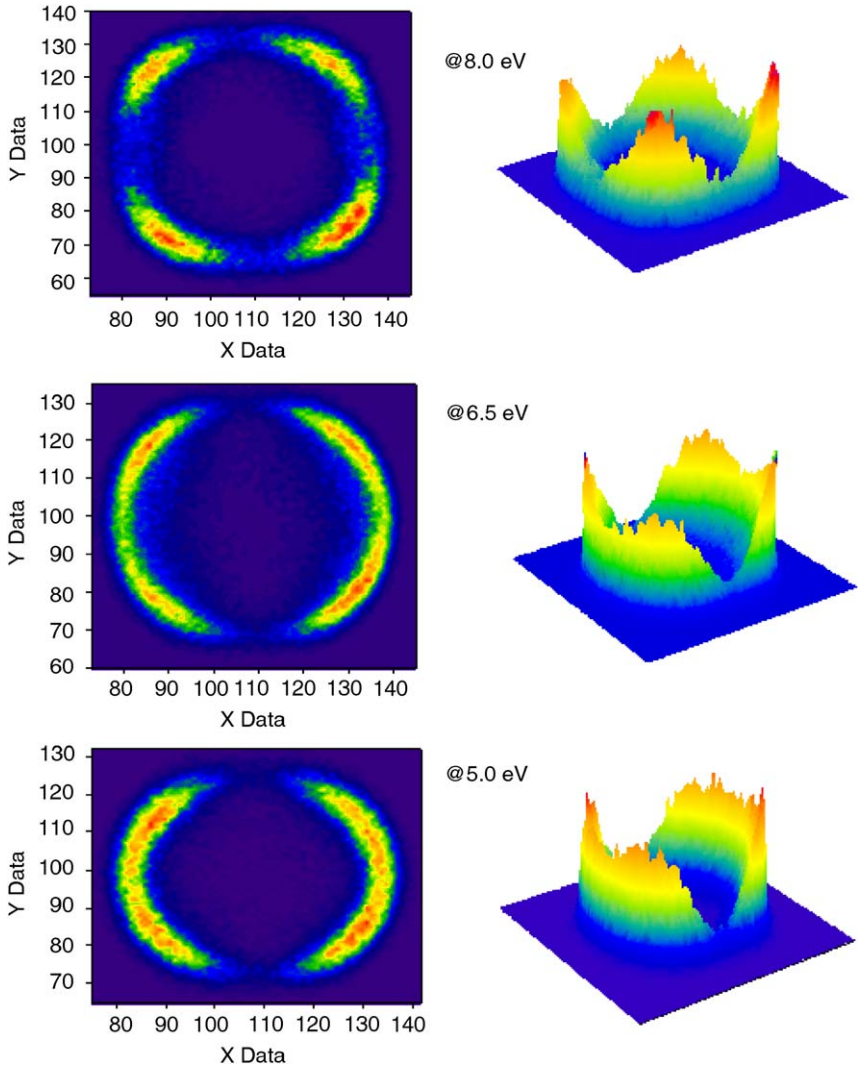

Fig. 4. Time sliced velocity map images of O^- from dissociative attachment to O_2 at different electron energies. The left panel shows the two-dimensional pattern we obtained after time slicing. Red color shows increasing intensity and blue shows least intensity. The electron beam direction is vertically down. The right panel shows the corresponding 3-d distribution with intensity as the z-axis. These distributions have been rotated through 35° in the counter clockwise direction for clarity.

the electrostatic lens the diameter of the ring is not linear with speed and hence needs to carry out a calibration to obtain quantitative information on kinetic energy. However, the cylindrical symmetry of the electrostatic lens ensures that the angular distributions are unaffected. The velocity map images clearly show most of the intensity to be distributed away from the forward and backward directions of the electron beam. Also as the electron energy increases, the intensity distribution becomes more pronounced towards the center (45°) of each quadrant. Another change noticeable is the increase in the intensity in the forward and backward angles as the electron energy is increased. The polar plots of these distributions at 10° interval are given in Fig. 5. The symmetry of the data about 180° show that the VMI set up is functioning satisfactorily.

In Fig. 6 we provide a comparison with the existing data. Though the energies are slightly different, it appears that there is good agreement within the two sets of data. However, the previous data seem to drop off slightly faster towards the backward and forward angles. Whereas our data appear to drop off slowly and reach finite values at 0° and 180°. In terms of the physics of the DA process this has significant implications. The previous data was fitted for contribution arising from a single negative ion resonant state, $^2\prod_u$, to the DA process (Van Brunt and Kieffer, 1970) using the functional form proposed by O'Malley and Taylor (1968). The corresponding expression, $I(k,\theta,\varphi) = |\sin\theta + 5\beta' \sin\theta\cos^2\theta|^2$, with β' being energy dependent constant, was found to give the best fit to the data. This expression cannot have nonzero values in the forward and backward directions. This implies that our measurements are pointing to the presence of an additional negative ion resonant state contributing to the DA process. The electron scattering measurements (Wong et al., 1973; Allan, 1995; Noble et al., 1996) have indicated the presence of a $^4\sum_u^-$ state in order to explain the excitation of very high lying vibrational levels of the ground state of O_2. However, it has been unclear why this state was not seen in the earlier angular distribution measurements on O^-. We believe that this may have been due to the difficulties involved in making measurements at angles closer to the forward and backward directions, including correction for the

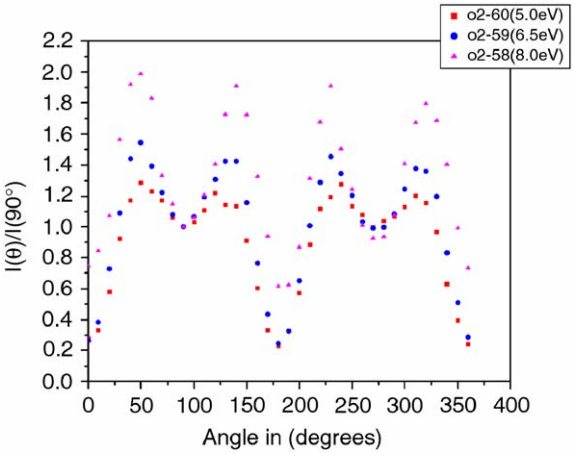

Fig. 5. Polar plots of the angular distributions at different electron energies of O^- from dissociative attachment to O_2. The distributions have been normalized at 90°. The squares, circles and triangles are the data at electron energies of 5.0, 6.5 and 8.0 eV, respectively.

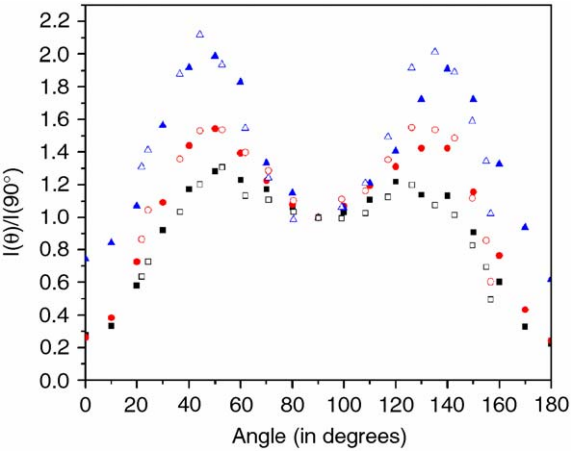

Fig. 6. Comparison of the present data on angular distribution of O^- from dissociative attachment to O_2 with previous results obtained using conventional technique. The filled squares, circles and triangles are the data at electron energies of 5.57, 6.70 and 7.80 eV, respectively, from Van Brunt and Kieffer (1970) and the open squares, circles and triangles are the present data at electron energies 5.0, 6.5 and 8.0 eV, respectively.

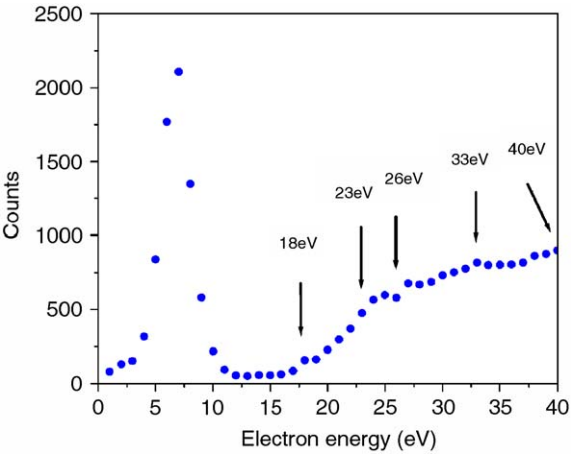

Fig. 7. O^- ion yield curve from O_2 up to 40 eV. The velocity map images were obtained at the energies indicated.

effective solid angle. Also measurements could not be made in the entire 2π range as we have done now. Thus, we believe that the nonzero cross-sections that we see in the forward and backward directions are primarily due to the $^4\sum_u^-$ state of O_2^-. This conclusion also points to the importance of having measurements carried out in the forward and backward directions, which the present technique is capable of. A detailed analysis of the contribution from the $^2\prod_u$ state and the $^4\sum_u^-$ state as a function of electron energy is being carried out and will be presented elsewhere.

In Fig. 7 we present the O^- ion yield curve in a wider electron energy range covering both the DA and the dipolar dissociation channels. It has been noticed earlier (Rapp and Briglia, 1965) that the dipolar dissociation part has specific structure superimposed on the continuum in the 20–35 eV range. This structure was investigated using the kinetic energy and angular distribution measurements of the ions (Van Brunt and Kieffer, 1974). We carried out measurements in this energy range using the VMI set up. The velocity map images of O^- ions at a number of electron energies indicated in Fig. 7 were obtained and they are shown in Fig. 8. The images show a central distribution that seems to be isotropic and present at all electron energies. We also see a broad annular distribution with a hexagonal pattern whose intensity is dependent on the electron energy. The kinetic energy distribution for O^- ions from this process has been shown to have a maximum at zero energy followed by a peak just below 2 eV and another one at 3.5 eV with a long tail extending up to 8 eV as the electron energy is increased (Van Brunt and Kieffer, 1974). It is also seen that the intensity of the 3.5 eV peak and the long tail increases with electron energy. With enough resolution, one should be able to see these kinetic energy distributions in the VMI data. In our data obtained up to 40 eV, we are able to see clearly only the zero energy distribution and another high-energy distribution. We believe that this distribution which shows strong anisotropy may correspond to the 2 eV peak seen in the kinetic energy spectra earlier (Van Brunt and Kieffer, 1974). We may be missing the higher energy distribution since the experiment was optimized for lower energy ions corresponding to the DA process.

The angular distributions corresponding to the observed ring pattern in the VMI at various energies are given in Fig. 9. The distributions appear to follow what has been reported earlier, with a minimum at 90° and maxima at 0° and 180°. For energies between 20 and 30 eV there appear two smaller peaks at about 65° and 115°. These intermediate peaks are sensitive to electron energy and has been explained as due to the expected deviation from the dipolar form of the scattering amplitude close to the excitation thresholds (Van Brunt and Kieffer, 1974). We note that there are some small differences between the present and the previous angular

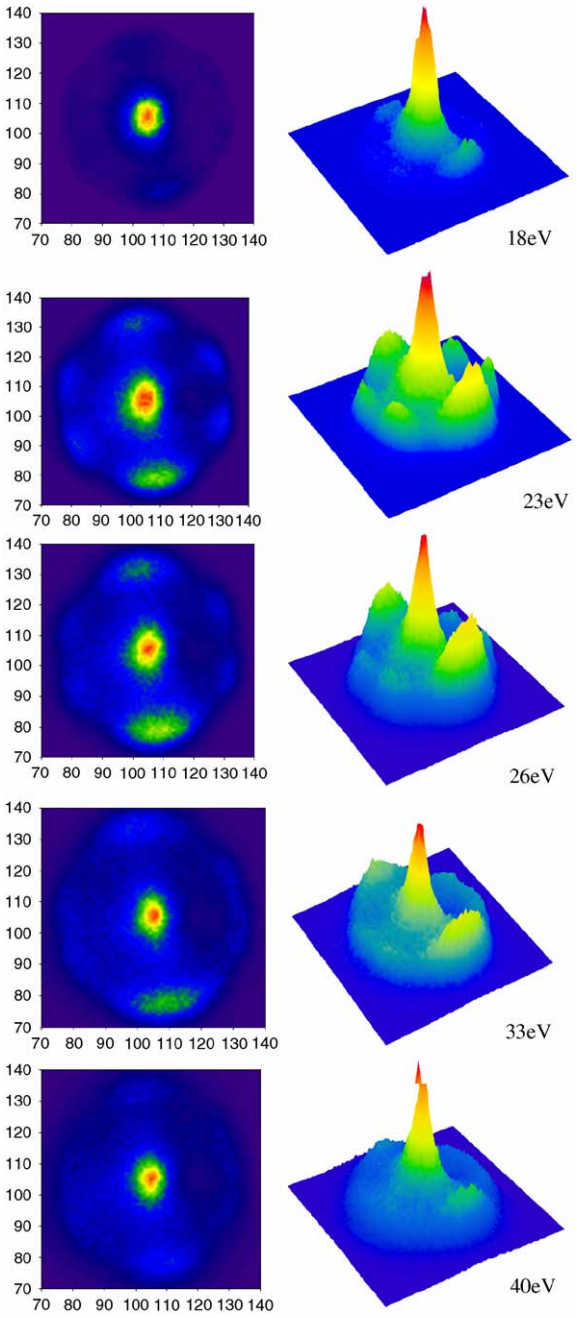

Fig. 8. Time sliced velocity map images of O^- from dipolar dissociation of O_2 at different electron energies. The left panel shows the two-dimensional pattern we obtained after time slicing. Red color shows increasing intensity and blue shows least intensity. The electron beam direction is nearly vertically down. The right panel shows the corresponding 3-d distribution with intensity as the z-axis. These distributions have been rotated through 40° in the counter clockwise direction for clarity.

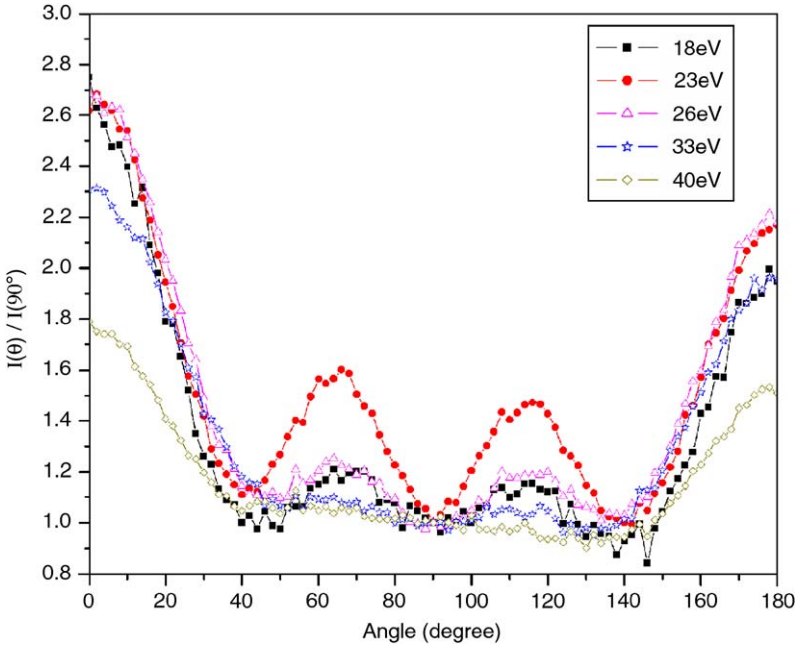

Fig. 9. Angular distribution of O^- ions from dipolar dissociation of O_2 at different energies. The data have been normalized at 90°.

distribution data related to the energies at which the maximum anisotropy occurs, the degree of anisotropy and the more pronounced forward–backward asymmetry. The reduction in the anisotropy may be explained as due to the wider band of ion energy we have selected for analysis. It is not clear at present the reasons for the other differences. We wish to point out that despite these differences and the inability to observe the higher energy ions, the VMI technique appears to be a suitable tool for studying the dipolar dissociation of molecules by electron impact.

To conclude, we have demonstrated the use of VMI technique for low-energy electron collision studies. The measurements on DA to O_2 have demonstrated the importance as well as advantages of this technique over the conventional one, particularly in its ability to obtain angular distribution data in the entire 2π range of angles. The preliminary measurements on dipolar dissociation using this technique have shown that it could be used for studying some of the auto-ionizing states of molecules, which decay through dissociation instead of electron emission.

Acknowledgment

We acknowledge with thanks A. Chatterjee, V.M. Nanal and R. Ramachandran for their help in setting up the data acquisition system. V.S. Prabhudesai and D. Nandi acknowledge the TIFR Alumni Association scholarship from TIFR Endowment fund.

References

Allan, M., 1995. Measurement of absolute differential cross sections for vibrational excitation of O_2 by electron impact. J. Phys. B: At. Mol. Opt. Phys. 28, 5163–5175.

Amitay, Z., Zajfman, D., 1997. A new type of multiparticle three-dimensional imaging detector with subnanosecond time resolution. Rev. Sci. Instrum. 68, 1387–1392.

Baguenard, B., Wills, J.B., Pagliarulo, F., Lépine, F., Climen, B., Barbaire, M., Clavier, C., Lebeault, M.A., Bordas, C., 2004. Velocity-map imaging electron spectrometer with time resolution. Rev. Sci. Instrum. 75, 324–328.

Bapat, B., Krishnakumar, E., 1994. Capillary array as an effusive molecular beam source for high resolution recoil ion momentum spectrometry. Z. Phys. D 31, 1–3.

Bapat, B., Krishnakumar, E., 1995. Effusive molecular beam from a capillary array for improved resolution time-of-flight and collision spectrometry. Rapid Commun. Mass Spectrom. 9, 199–202.

Becker, K.H., McCurdy, C.W., Orlando, T.M, Rescigno, T.N., 2000. Current status and future perspectives of electron interactions with molecules, clusters, surfaces and interfaces. http://attila.stevens-tech.edu/physics/People/Faculty/Becker/EDP

Berkowitz, J., 1979. Photoabsorption, Photoionization and Photoelectron Spectroscopy. Academic Press, New York.

Boudaiffa, B., Cloutier, P., Hunting, D., Huels, M.A., Sanche, L., 2000. Resonant formation of DNA strand breaks by low-energy (3–20 eV) electrons. Science 287, 1658–1660.

Chandler, D.W., Houston, P.L., 1987. Two-dimensional imaging of state-selected photodissociation products detected by multiphoton ionization. J. Chem. Phys. 87, 1445–1447.

Chatterjee, A. http://www.tifr.res.in/~pell/lamps.html

Diez, M.R., Schmidt-Böcking, H., Dörner, R., 2004. Complete photo-fragmentation of the deuterium molecule. Nature 431, 437–440.

Dinu, L., Eppink, A.T.J.B., Rosca-Pruna, F., Offerhaus, H.L., van der Zande, W.J., Vrakking, M.J.J., 2002. Application of a time-resolved event counting technique in velocity map imaging. Rev. Sci. Instrum. 73, 4206–4213.

Dörner, R., Mergel, V., Spielberger, L., Achler, M., Kayyat, Kh., Vogt, T., Bräuning, H., Jagutzki, O., Weber, T., Ullrich, J., Moshammer, R., Unverzagt, M., Schmitt, W., Khemliche, H., Prior, M.H., Cocke, C.L., Feagin, J., Olson, R.E., Schmidt-Böcking, H., 1997. Kinematically complete experiments using cold target recoil ion momentum spectroscopy. Nucl. Instrum. Methods B 124, 225–231.

Dunn, G.H., 1962. Anisotropies in angular distribution of molecular dissociation products. Phys. Rev. Lett. 8, 62–64.

Eppink, A.T.J.B., Parker, D.H., 1997. Velocity map imaging of ions and electrons using electrostatic lenses: application in photoelectron and photofragment ion imaging of molecular oxygen. Rev. Sci. Instrum. 68, 3477–3484.

Gebhardt, C.R., Rakitzis, T.P., Samartzis, P.C., Ladopoulos, V., Kitsopoulos, T.N., 2001. Slice imaging: a new approach to ion imaging and velocity mapping. Rev. Sci. Instrum. 72, 3848–3853.

Helm, H., Bjerre, N., Dyer, M.J., Huestis, D.L., Saeed, M., 1993. Images of photoelectrons formed in intense laser fields. Phys. Rev. Lett. 70, 3221–3224.

Krishnakumar, E., Nagesha, K., 1992. Dissociative attachment of electrons to CS_2. J. Phys. B: At. Mol. Opt. Phys. 25, 1645–1660.

Krishnakumar, E., Srivastava, S.K., 1992. Cross-sections for electron impact ionization of O_2. Int. J. Mass Spectrom. Ion Process. 113, 1–12.

Krishnakumar, E., Kumar, S.V.K., Rangwala, S.A., Mitra, S.K., 1997. Dissociative-attachment cross sections for excited and ground electronic states of SO_2. Phys. Rev. A 56, 1945–1953.

Noble, C.J., Higgins, K., Wöste, G., Duddy, P., Burke, P.G., Teubner, P.J.O., Middleton, A.G., Brunger, M.J., 1996. Resonant mechanisms in the vibrational excitation of ground state of O_2. Phys. Rev. Lett. 76, 3534–3537.

O'Malley, T.F., Taylor, H.S., 1968. Angular dependence of scattering products in electron–molecule resonant excitation and in dissociative attachment. Phys. Rev. 176, 207–221.

Rangwala, S.A., Kumar, S.V.K., Krishnakumar, E., 2001. Dissociative electron attachment to electronically excited CS_2. Phys. Rev. A 64, 012707.

Rapp, D., Briglia, D.D., 1965. Total cross sections for ionization and attachment in gases by electron impact. II. Negative-ion formation. J. Chem. Phys. 43, 1480–1489.

Rottke, H., Trump, C., Wittmann, M., Korn, G., Sandner, W., Moshammer, R., Dorn, A., Schröter, C.D., Fischer, D., Crespo Lopez-Urrutia, J.R., Neumayer, P., Deipenwisch, J., Höhr, C., Feuerstein, B., Ullrich, J., 2002. Coincident fragment detection in strong field photo ionization and dissociation of H_2. Phys. Rev. Lett. 89, 013001.

Schulz, M., Moshammer, R., Fischer, D., Kollmus, H., Madison, D.H., Jones, S., Ullrich, J., 2003. Three-dimensional imaging of atomic four-body processes. Nature 422, 48–50.

Townsend, D., Minitti, M.P., Suits, A.G., 2003. Direct current slice imaging. Rev. Sci. Instrum. 74, 2530–2539.

Ullrich, J., Dörner, R., Lencinas, S., Jagutzki, O., Schmidt-Böcking, H., Buck, U., 1991. Recoil-ion momentum spectroscopy. Nucl. Instrum. Methods B 61, 415–422.

Van Brunt, R.J., Kieffer, L.J., 1970. Angular distribution of O^- from dissociative electron attachment to O_2. Phys. Rev. A 2, 1899–1904.

Van Brunt, R.J., Kieffer, L.J., 1974. Electron energy dependence of the energy and angular distribution of O^- from dissociative ion pair formation in O_2. J. Chem. Phys. 60, 3057–3063.

Weber, T., Czasch, A.O., Jagutzki, O., Müller, A.K., Mergel, V., Kheifets, A., Feagin, J., Rotenberg, E., Meigs, G., Prior, M.H., Daveau, S., Landers, A.L., Cocke, C.L., Osipov, T., Schmidt-Böcking, H., Dörner, R., 2004. Fully differential cross sections for photo-double-ionization of D_2. Phys. Rev. Lett. 92, 163001.

Whitaker, B. (Ed.), 2003. Imaging in Molecular Dynamics. Cambridge University Press, Cambridge.

Wong, S.F., Boness, M.J.W., Schulz, G.J., 1973. Vibrational excitation of O_2 by electron impact above 4 eV. Phys. Rev. Lett. 31, 969–972.